

SCIENTIFIC REPORTS



OPEN

Comparative morphology and transcriptome analysis reveals distinct functions of the primary and secondary laticifer cells in the rubber tree

Deguan Tan¹, Xiaowen Hu², Lili Fu¹, Anuwat Kumpeangkeaw^{1,3}, Zehong Ding¹, Xuepiao Sun¹ & Jiaming Zhang¹

Laticifers are highly specialized cells that synthesize and store natural rubber. Rubber trees (*Hevea brasiliensis* Muell. Arg.) contain both primary and secondary laticifers. Morphological and functional differences between the two types of laticifers are largely unknown, but such information is important for breeding and cultivation practices. Morphological comparison using paraffin sections revealed only distribution differences: the primary laticifers were distributed randomly, while the secondary laticifers were distributed in concentric rings. Using isolated laticifer networks, the primary laticifers were shown to develop via intrusive “budding” and formed necklace-like morphology, while the secondary laticifers developed straight and smooth cell walls. Comparative transcriptome analysis indicated that genes involved in cell wall modification, such as pectin esterase, lignin metabolic enzymes, and expansins, were highly up-regulated in the primary laticifers and correspond to its necklace-like morphology. Genes involved in defense against biotic stresses and rubber biosynthesis were highly up-regulated in the primary laticifers, whereas genes involved in abiotic stresses and dormancy were up-regulated in the secondary laticifers, suggesting that the primary laticifers are more adequately prepared to defend against biotic stresses, while the secondary laticifers are more adequately prepared to defend against abiotic stresses. Therefore, the two types of laticifers are morphologically and functionally distinct.

Natural rubber consists primarily of isoprene (cis-1,4-polyisoprene) polymers, and is used in a diverse products, such as tires, condoms, shoes, dampening and insulating elements, and approximately 40,000 other products¹. Due primarily to its molecular structure and high molecular weight (>1 million Da)^{2–4}, natural rubber has a large stretch ratio, high resilience, abrasion resistance, efficient heat dispersion, impact resistance, and extreme water-proof characteristics. This combination of high-performance properties cannot easily be mimicked by artificially produced polymers^{1,5}, and natural rubber still accounts for more than 30% of the 15 billion kilograms of rubber produced annually⁶.

Natural rubber is synthesized in highly specialized plant cells, known as laticifers or latex vessels. Approximately 12,500 plant species among 22 families produce rubber in laticifers⁷; however, the rubber tree (*Hevea brasiliensis* Muell. Arg.) is the only source of commercial natural rubber in the global market^{8,9}. The economic importance of natural rubber has prompted investigations into its biosynthesis. Both the primary and the secondary laticifers in the rubber tree produce rubber, but only the secondary laticifers in the bark of mature trees are economically exploited. Primary laticifers are not tapped in production practice, because the primary laticifers are mainly present in the bark of young shoots or stems but disappear in the bark of the tree trunk

¹Institute of Tropical Bioscience and Biotechnology, MOA Key Laboratory of Tropical Crops Biology and Genetic Resources, Hainan Bioenergy Center, CATAS, Xueyuan Road 4, Haikou, Hainan Province, 571101, China. ²Zhanjiang Experimental Station, CATAS, West Libration Road 20, Zhanjiang, Guangdong Province, 524013, China. ³Song Khla Rubber Research Centre, Department of Agriculture, Ministry of Agriculture and Cooperatives, Had Yai, Song Khla, 90110, Thailand. Deguan Tan, Xiaowen Hu and Lili Fu contributed equally to this work. Correspondence and requests for materials should be addressed to J.Z. (email: zhangjiaming@itbb.org.cn)

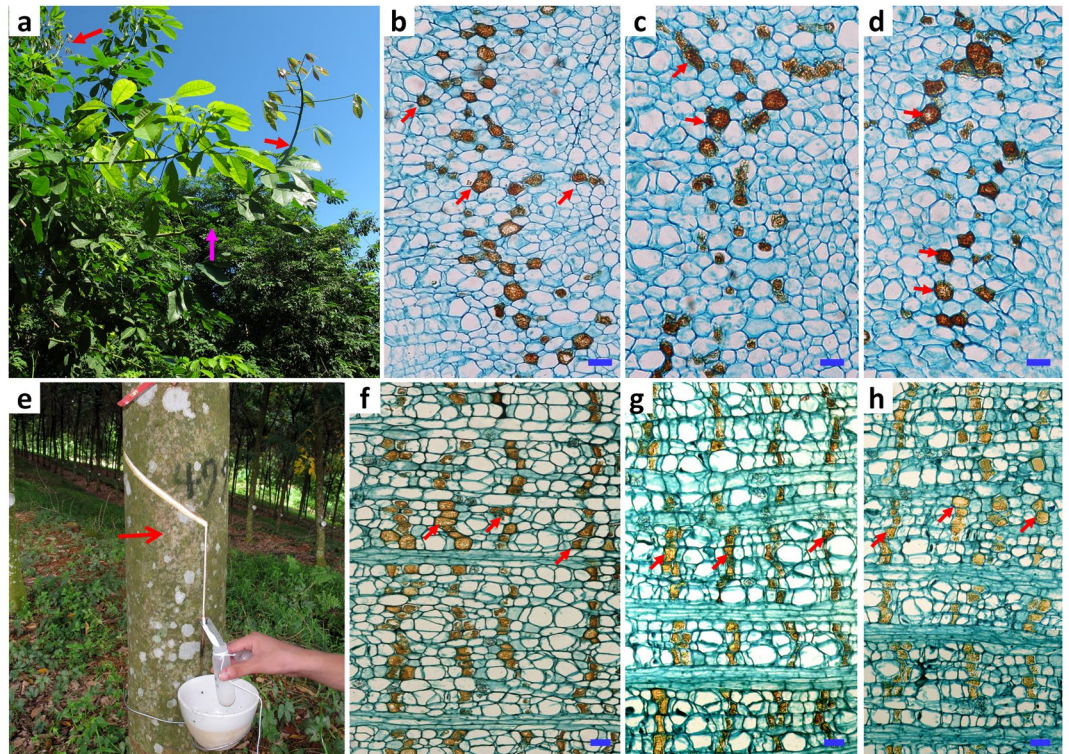


Figure 1. A comparison of the primary and the secondary laticifer cells in cross-sections. (a) Canopy of rubber tree clone RY7-33-97 (7-years old). Red arrows indicate the young shoots where the primary latex for RNA isolation and the bark samples for histological observation were collected, and the pink arrow indicates the region containing both the primary and the secondary laticifer cells. (b–d) Representative cross-sections of the bark of young shoots selected from three biological replicates. Red arrows indicate the primary laticifer cells. The scale bar represents 20 μm ; (e) A rubber tree trunk showing the latex in the first tapping. The red arrow indicates where the bark sample was collected for anatomical analysis. (f–h) Representative cross-sections of the bark from tree trunks showing the secondary laticifer cells; The scale bar represents 20 μm .

during maturation (>6 years old)¹⁰. The primary laticifers are differentiated from the meristematic zones, while the secondary laticifers are differentiated from vascular cambium and are present in rings parallel to the vascular cambium in the secondary phloem of the trunk.

The number of secondary laticifer rings varies in different rubber tree clones, which are propagated by bud grafting and are used for commercial cultivation. Clones with more secondary laticifer rings typically have a higher rubber yield^{8,11,12}. Therefore, the secondary laticifers have become the focus of rubber tree researchers. By comparison, less research has focused on the primary laticifer cells. The number and latex-producing potential of the primary laticifer cells have been used for early predictions of rubber yield of hybrid clones to shorten the breeding cycle^{13,14}; however, these predictions have been reported to be inaccurate^{12,15}. The relationship and/or correlation between the primary and the secondary laticifers are important for breeding and cultivation practices, but these relationships need to be thoroughly investigated. In this study, we compared the morphological differences of the primary and the secondary laticifers by investigating isolated laticifer networks using a new technology instead of conventional paraffin sections, and revealed significant morphological differences. Additionally, comparative transcriptome analysis revealed functional differences between the two types of laticifers.

Results

Morphological comparison of the primary and the secondary laticifers in rubber tree. The newly emerged young shoots of rubber trees contained only the primary laticifer cells (Fig. 1a–d), while the tree trunk contained only the secondary laticifers (Fig. 1e–h). Following staining of cross-sections with iodine bromide solution, no obvious morphological differences between single cells of the primary and the secondary laticifers were observed, except for the distribution pattern. The primary laticifer cells were distributed more or less at random in the phloem (Fig. 1b–d). In contrast, the secondary laticifer cells were distributed in rows and formed multiple rings around the trunk (Fig. 1f–h).

The primary and the secondary laticifer networks were partially isolated from bark, along with a few parenchyma cells to be used as reference cells (Fig. 2). The laticifer cells were easily identified by their dark color due to the rubber content in the absence of staining. The primary laticifer cells were differentiated from meristematic cells, and the initial laticifer tubes were thin, straight, un-branched, and often non-articulated (Fig. 2a,b). During development, primary laticifer tubes initiated intrusive growth and expanded towards the neighboring parenchyma cells at discrete locations (Fig. 2c), and eventually, the tubes formed necklace-like structures (Fig. 2d,e).

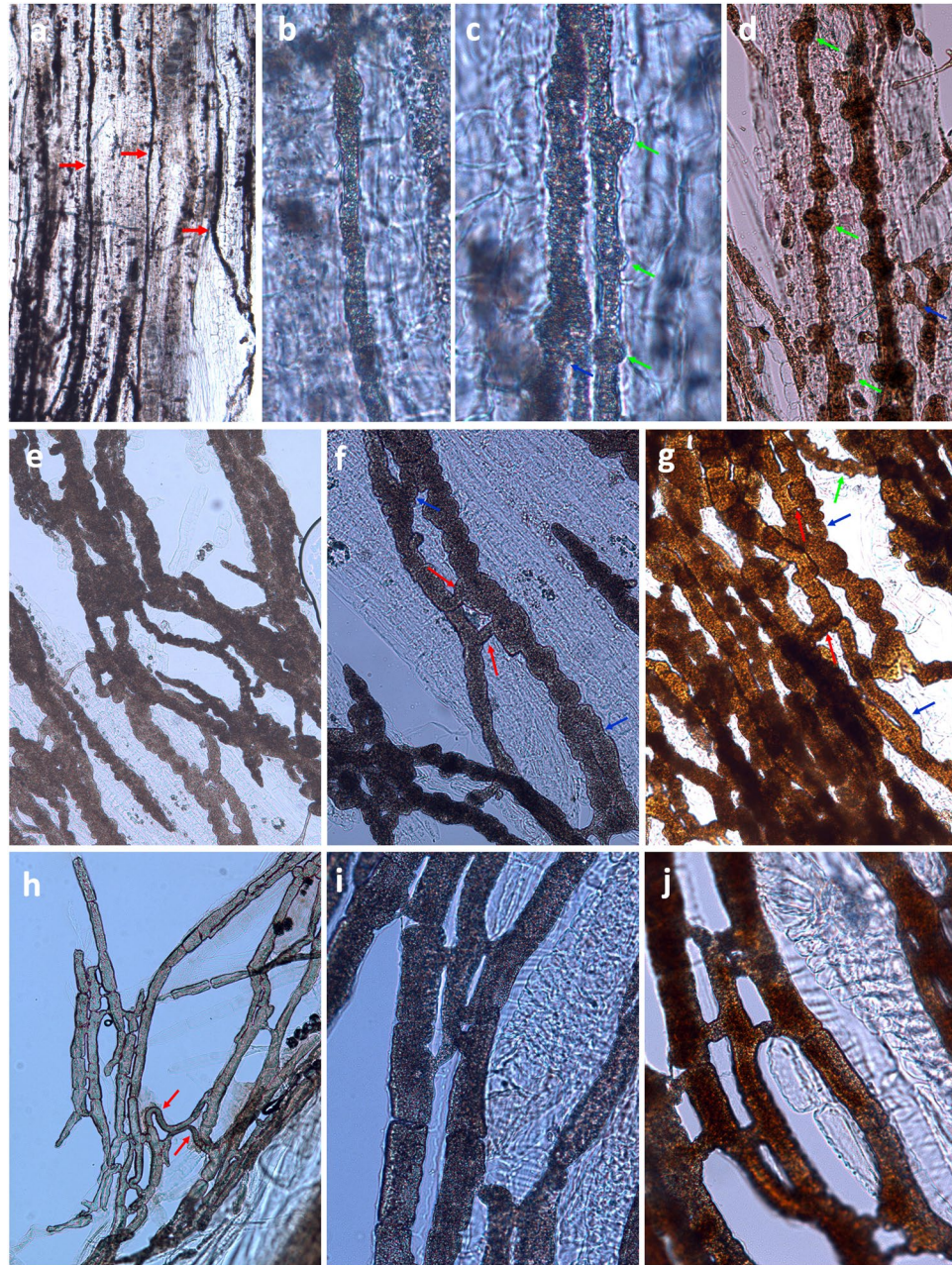


Figure 2. Laticifer cells partially isolated from the rubber tree bark. (a–g) Primary laticifers unstained (a–c and e–f) or stained with iodine and bromine solution (d,g); (h–j) secondary laticifer cells unstained (h and i) or stained with iodine and bromine solution (j). Yellow arrows indicate primary laticifers; green arrows indicate intrusive growth by “budding;” blue arrows indicate laticifer branches; red arrows indicate linkage tubes between two laticifers.

Laticifer branches were also formed at this time (Fig. 2c,d). The tubes were then inflated at additional locations and formed dense necklace-like structures (Fig. 2e). The neighboring “beads” were merged gradually to form laticifer tubes of larger diameter, and ultimately, neighboring tubes were connected by bridges to form a laticifer network (Fig. 2e,f,g).

The secondary laticifer cells originated from cambium cells. These laticifers were articulated and had thick, straight, and smooth cell walls (Fig. 2h,i,j). The neighboring tubes were anastomosed by short bridges, and some distant and parallel tubes were joined by specialized laticifer cells that grew transversely in the bark (Fig. 2h). Each cell was joined to two or more cells of the neighboring tubes at different locations (Fig. 2h,i,j).

Sequencing, assembling, and enrichment analysis of differentially expressed genes (DEGs). To understand the distinct morphology of the primary and the secondary laticifer vessels, the transcriptomes of these cell types of virgin RY7-33-97 rubber trees were sequenced using the Illumina paired-end

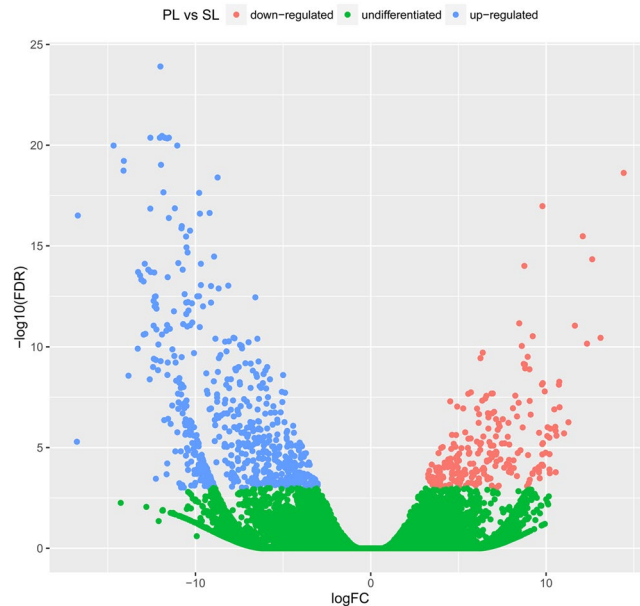


Figure 3. Differential expression analysis of unigenes in the primary laticifers (PL) versus the secondary laticifers (SL). The LogFC (log₂ Fold Change) is used as the x-axis and $-\log_{10}$ FDR (False Discovery Rate) is used as the y-axis. The total number of unigenes is 70,933. Of those 70,089 were not DEGs (cut-off FDR ≤ 0.001 , highlighted in green), 597 unigenes were up-regulated in PL (highlighted in blue), and 247 unigenes were down-regulated (highlighted in red).

sequencing method with three biological replicates. Totally six RNA-seq libraries were generated and more than 312 million raw reads were obtained. After trimming adaptors and removing reads with low quality, 262 million (84.0%) clean reads were remained and were used to construct de novo transcription profiles with the Trinity software^{16,17}. In total, 131,078 transcripts (N50 = 1,406) and 103,704 unigenes were identified (Supplementary Table S1). Sample clustering of gene expression indicated that replicates of the same tissue were grouped together (Supplementary Fig. S1). PCA plot analysis indicated that the replicates of PL and SL samples were well separated (Supplementary Fig. S2). These results support the uniformity and reliability of the transcriptome data across replicates. The gene expression data was normalized with the trimmed mean of M values (TMM) method and the abundance was calculated as transcripts per million transcripts (TPM). Filtering of the expressed genes with $\text{TPM} \leq 1$, we identified 70,933 unigenes. A total of 48,780 (68.77%) unigenes were hit and functionally annotated by BLAST against publicly available databases using a cutoff E-value $< 1.00\text{E-}5$ (Supplementary Table S2), in which the databases SwissProt, nt, GO, and TrEMBL accounted for 39.68%, 50.29%, 41.02%, and 63.29% of the annotation, respectively (Supplementary Table S3). In total, 844 DEGs were identified using edgeR, an R program package, with an adjusted *p*-value cut-off for false discovery rate (FDR) ≤ 0.001 and $|\log_2\text{Ratio}| \geq 2$ ¹⁸. Of these DEGs, 597 were up-regulated and 247 were down-regulated in the primary laticifers compared to the levels in the secondary laticifers (Fig. 3), indicating that the gene expression profiles were significantly changed during the transition of these two types of laticifer cells.

To gain insight into the pathways that were altered during the transition between the primary and the secondary laticifers, the 844 DEGs were annotated and imported to MapMan for visualization. This analysis revealed that most genes involved in cell wall synthesis, degradation, and modification were up-regulated as were genes involved in lignin biosynthesis, amino acid metabolism, redox, and secondary metabolism of isoprenoids, while genes related to trehalose biosynthesis, lipid degradation, and gluconeogenesis were down-regulated in the primary laticifers compared to the secondary laticifers (Supplementary Fig. S3). Gene ontology (GO) analysis also showed similar results (Supplementary Table S4). In total, 142 enriched GO categories were identified, and 94 of these were enriched in the primary laticifers, while 50 were enriched in the secondary laticifers (Supplementary Table S4). Two of these (GO:0050267, rubber cis-polyprenylcistransferase activity; GO:0080167, response to karrikin) were commonly enriched in both the primary and the secondary laticifers (Supplementary Table S4).

Genes involved in cell development and cell wall modification are up-regulated in the primary laticifers.

DEGs involved in cell development and cell wall modification were up-regulated in the primary laticifers (Supplementary Table S4). These genes were clustered into the sub-categories cell wall modification, pectin catabolic process, plant-type cell wall, cell wall macromolecule catabolic process, lignin metabolic process, regulation of cell size, pollen tube guidance, and syncytium formation (Fig. 4). The most significant DEGs belonged to pectin catabolic processes and included eight unigenes that encode pectinesterase (Fig. 4). Of these eight, U34182c1g1 was the most differentially expressed. The TPM values of U34182c1g1 in the primary and the secondary laticifers were 4,294 and 1, respectively. Pectinesterase is a ubiquitous cell-wall-associated enzyme that facilitates pectin de-esterification, cell wall modification, and subsequent breakdown^{19,20}. The over-expression

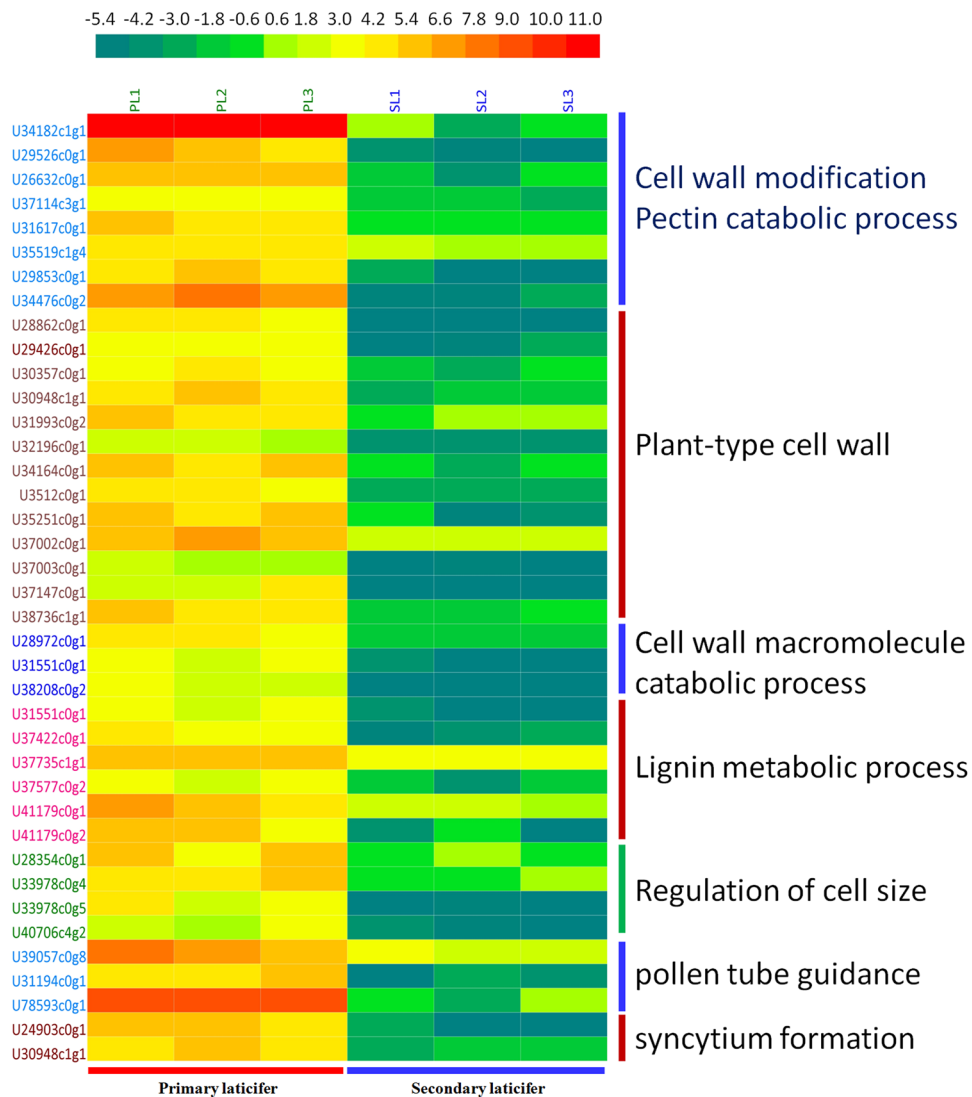


Figure 4. Heatmap of DEGs involved in cell growth and cell wall modification. The expression levels of DEGs in TPM were compiled with Excel 2007, normalized using a log₂ base method, and exported to the HemI toolkit¹²⁴. The Heatmap was generated using the default parameters. The expression levels are presented as different colors, and the values are defined in the scale bar. PL, the primary laticifers; SL, the secondary laticifers.

of pectinesterases in the primary laticifers may play a major role in intrusive growth, including the formation of necklace-like structures and subsequent cell expansion of the primary laticifers (Fig. 2).

A total of thirteen DEGs that were up-regulated in the primary laticifers were clustered into plant-type cell wall (Fig. 4). These DEGs encoded berberine bridge enzymes, methyltransferases, class III peroxidases, alpha-expansin, RALF-like protein, subtilisin-like protease, pectin acetyltransferase, alpha-glucosidase, vacuolar invertase, and heparanase-like protein. Six DEGs were clustered in the lignin metabolic process and included laccase, transaldolase, chitinase-like protein, and three xylem serine proteinase genes. Four DEGs were clustered in the regulation of cell size, and these genes encoded O-glycosyl hydrolases family 17, two metallothionein 3-like proteins, and WALLS ARE THIN 1 (WAT1)-like protein. Other DEGs that were up-regulated in the primary laticifers included three DEGs in the cell wall macromolecule catabolic process and three DEGs in the pollen tube guidance and regulation of pollen growth. An annexin-like protein (U39057c0g8) with homologs that have been implicated in regulation of pollen tube and fiber growth^{21, 22} in Arabidopsis and cotton, respectively, was highly up-regulated in the primary laticifers. Annexins interact with cell membrane components that are relevant to the structural organization of the cell, and these proteins are involved in cell shape, intracellular signaling, and growth control and act as atypical calcium channels^{23, 24}. Therefore, the growth of the primary laticifer cells may share some similarities with pollen tubes and fibers.

Interestingly, two DEGs involved in syncytium formation were up-regulated in the primary laticifer (Fig. 4). One (U24903c0g1) encoded an expansin B3-like protein, and the other encoded an alpha-expansin 4-like protein. Expansins are involved in extensive cell wall modification during interactions between nematodes and host^{25–28}.

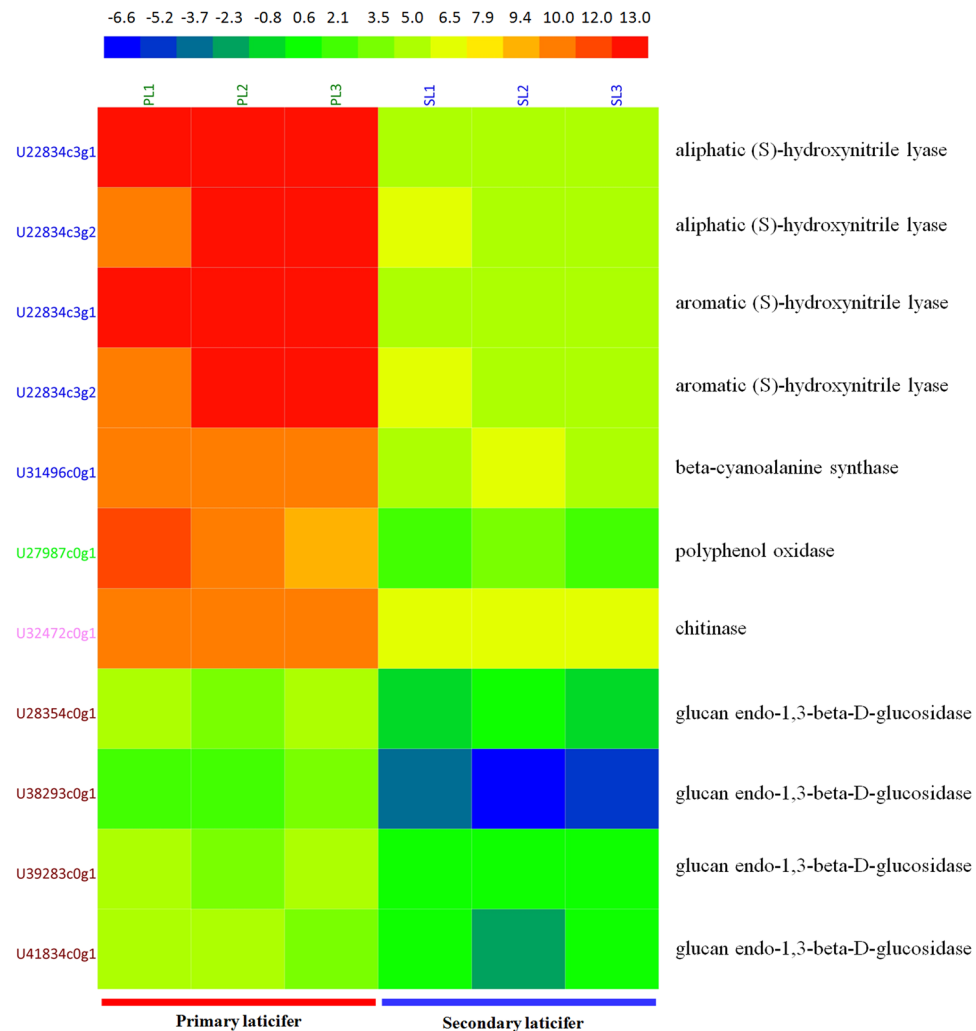


Figure 5. Heatmap of DEGs involved in biotic stresses. The expression levels of DEGs in TPM were compiled with Excel 2007, normalized using a log₂ base method, and exported to the HemI toolkit¹²⁴. The Heatmap was generated using the default parameters. The expression levels are presented in different colors, and the values are defined in the scale bar. PL, the primary laticifers; SL, the secondary laticifers.

Taken together, numerous DEGs that are related to cell wall modification and/or cell development were up-regulated in the primary laticifers, resulting in the active intrusive growth of the primary laticifer cells and the formation of their necklace-like morphology.

Genes involved in defense against biotic stresses are up-regulated in the primary laticifer. The second most significant finding was the strong up-regulation of genes involved in defense against biotic stresses in the primary laticifers. These up-regulated genes included (S)-hydroxynitrile lyase, beta-cyanoalanine synthase, polyphenol oxidase, chitinase, and glucanase (Fig. 5), suggesting that the young tissue was prepared more adequately to defend attacks by herbivorous animals and pathogens.

The most significant up-regulated DEGs in the primary laticifers encoded (S)-hydroxynitrile lyases (EC4.1.2.47, HNL), including two aliphatic (S)-hydroxynitrile lyases (U22834c3g1, U22834c3g2) and two aromatic (S)-hydroxynitrile lyases (U22834c3g1, U22834c3g2). The TPM values of these genes were more than 17,000 in the primary laticifers, a value that is 200 to 400-fold higher than that in the secondary laticifers. HNL catalyzes the hydrolysis of (S)-hydroxynitriles and releases the toxin cyanide. The latter serves as a defense mechanism against herbivores and microbial attack in plants²⁹. This report is the first to describe high expression of hydroxynitrilases in the primary laticifers. A hydroxynitrilase gene was originally cloned from the leaves of the rubber tree³⁰. However, another DEG (U31496c0g1) encoded a beta-cyanoalanine synthase, which contributes to cyanide detoxification³¹. This DEG was up-regulated in the primary laticifers and had a TPM value of 2055.5, which is approximately 28-fold higher than that in the secondary laticifers (TPM = 72.9).

In addition, a polyphenol oxidase (PPO, U27987c0g1) was also highly up-regulated in the primary laticifers with an average TPM value of 2180.4 compared to a value of 7.1 in the secondary laticifers (Fig. 5). PPO has been demonstrated to function as a defense mechanism against pest insects and pathogens³².

Chitinase and glucan endo-1,3-beta-D-glucosidase (EC3.2.1.39) are hydrolases that are well known for their antifungal activity. A chitinase gene (U32472c0g1) was transcribed at very high levels in the primary laticifers and accounted for more than 95% of the total chitinase transcription in the primary laticifers with a TPM value of 3004.2, which was approximately 21-fold higher than that in the secondary laticifers (TPM = 139.4; Fig. 5). This chitinase has 311 amino acid residues and has only two C-terminal amino acid differences compared with hevamine (AJ007701) in rubber tree³³. Five additional chitinase unigenes were also up-regulated in the primary laticifers; however, their expression levels were low (TPM < 100) compared to that of U32472c0g1. Thus, these genes were omitted from further analysis. None of the chitinase genes, however, were up-regulated in the secondary laticifers. Glucan endo-1,3-beta-D-glucosidase, also known as endo-1,3-beta-glucanase, laminarinase, and 3-beta-D-glucan glucanohydrolase, function in antifungal defense via degradation of fungal cell walls^{34,35}. More than 100 unigenes that were homologous to glucanase family members were identified in the laticifer transcriptomes, and of these, four were consistently up-regulated in the primary laticifers (FDR \leq 0.001; log₂Ratio \geq 2; Fig. 5). None of the glucanase genes were consistently up-regulated in the secondary laticifers.

Genes involved in the rubber biosynthesis pathway are mainly up-regulated in the primary laticifers. Natural rubber is composed of mainly high molecular weight cis-polyisoprene synthesized via sequential condensation of isopentenyl diphosphate (IPP)³⁶. IPP is synthesized via two pathways: the mevalonate (MVA) pathway, which occurs in the cytoplasm³⁷, and the 2-C-methyl-D-erythritol 4-phosphate (MEP) pathway, which occurs in the plastid³⁸. Almost all the enzymes involved in IPP synthesis were up-regulated in primary laticifer cells, except for the phosphomevalonate kinase (PMVK) gene (U39559c1g1) in the MVA pathway and the 2-C-methyl-D-erythritol 4-phosphate cytidylyltransferase (MCT) gene (U40439c1g1) in the MEP pathway (Fig. 6). Most genes that encode enzymes in the MEP pathway were transcribed at relatively low levels with TPM values < 20, except for 1-deoxy-D-xylulose 5-phosphate synthase (DXS, U38125c0) and 4-hydroxy-3-methylbut-2-en-1-yl diphosphate reductase (HDR, U28674c0g1), which had TPM values of approximately 90 in the primary laticifers (Fig. 6). The overall transcription levels of the genes in the conventional MVA pathway were much higher than those in the MEP pathway (Fig. 6). The most actively transcribed genes encoded key enzymes in the MVA pathway. These genes included hydroxymethylglutaryl coenzyme A synthase (HMGS, U38242c1g1), two hydroxymethylglutaryl coenzyme A reductases (HMGR, U32666c0g1 and U263c0), and acetyl coenzyme A acetyltransferase (AACT, U40809c3g2), with TPM values of 1600, 537, 489, and 1426, respectively, in the primary laticifer cells. These results suggest that the MVA pathway accounts for the majority of IPP biosynthesis.

Enzymes involved in post-IPP processes were also up-regulated in the primary laticifers (Fig. 6). Two unigenes (U31940c0g1 and U22231c0g1) that encode isopentenyl isomerase (IPI) were identified in both the primary and the secondary laticifers, and were up-regulated in the primary laticifers. The farnesyl diphosphate synthase (FDPS) family catalyzes the synthesis of farnesyl pyrophosphate (FPP), which subsequently serves as the priming substrate for the initiation of the prenyl chain. Thus, FDPS family members are crucial enzymes in the biosynthesis of rubber. Two FDPS family members, U40177c2g2 and U41662c1g1, were found to be up-regulated in the primary laticifers (Fig. 6). Furthermore, the cis-prenyltransferase (CPT) family, which is also known as *Hevea* rubber synthase (HRT), is crucial for integration of IPP units into the prenyl chain^{39,40}. U40757c3g5, which is the major transcript encoding CPT, was found to be up-regulated in the primary laticifers (Fig. 6).

Genes involved in abiotic stress responses are up-regulated in the secondary laticifers. DEGs that were up-regulated in the secondary laticifers (FDR \leq 0.001 and |Log₂Ratio(RS/RP)| \geq 2) were most related to abiotic stress responses, including transcription factors and/or signal receptors of brassinosteroid, karrikin, sucrose, and auxin. The most highly up-regulated transcription factors were a MADS-box transcription factor (U35197c0g1) and a homeobox-leucine zipper protein (U32937c1g1, Fig. 7). Other up-regulated factors included three WRKY superfamily proteins and eight auxin responsive proteins (Fig. 7). These DEGs may be related to the dormancy of the axillary buds in the tree trunk and may also be related to the dormancy of the secondary laticifers in untapped trees, resulting in the down-regulation of DEGs involved in rubber biosynthesis in the secondary laticifers (Fig. 6). Genes involved in rubber biosynthesis are indeed up-regulated by tapping⁴¹.

The trehalose-phosphate synthase (TPS) genes have been reported to enhance drought resistance^{42,43}. Two TPS (U29458c0g1 and U34155c0g1) genes were up-regulated in the secondary laticifers. A heat stress-responsive transcription factor C-1-like protein gene (U34335c0g1) was also up-regulated in the secondary laticifers. This protein homolog in *Arabidopsis* and rice is known to regulate the expression of heat shock proteins^{44,45}. Another DEG (U24674c0g1) encoding an asparaginase (EC 3.5.1.1) was also up-regulated in the secondary laticifers, and a homolog of this DEG (GmASP1) is known to be induced by cold stress in soybean⁴⁶.

Validation of representative DEGs by quantitative reverse-transcription polymerase chain reaction (qRT-PCR). To validate the RNA-seq results, 15 representative DEGs, including 10 up-regulated DEGs in the primary laticifers and five up-regulated DEGs in the secondary laticifers. Three reference genes that were stable in both laticifers (Supplementary Table S5) were selected for qRT-PCR analysis. The results indicated that the Log₂(PL/SL) values of all the 15 DEGs (where PL is the primary laticifers and SL is the secondary laticifers) were similar between qRT-PCR and RNA-seq results (Fig. 8) with a correlation coefficient R² of 0.876 (Supplementary Fig. S4), indicating that the RNA-seq comparative transcriptome analysis between the primary and the secondary laticifer cells was reliable.

Discussion

Comparison of laticifer paraffin sections versus laticifer isolation. We have compared the morphology of the primary and the secondary laticifers in both paraffin sections and via isolated laticifer networks. Paraffin sections are the traditional method widely used for studies of laticifer development in rubber tree¹⁰.

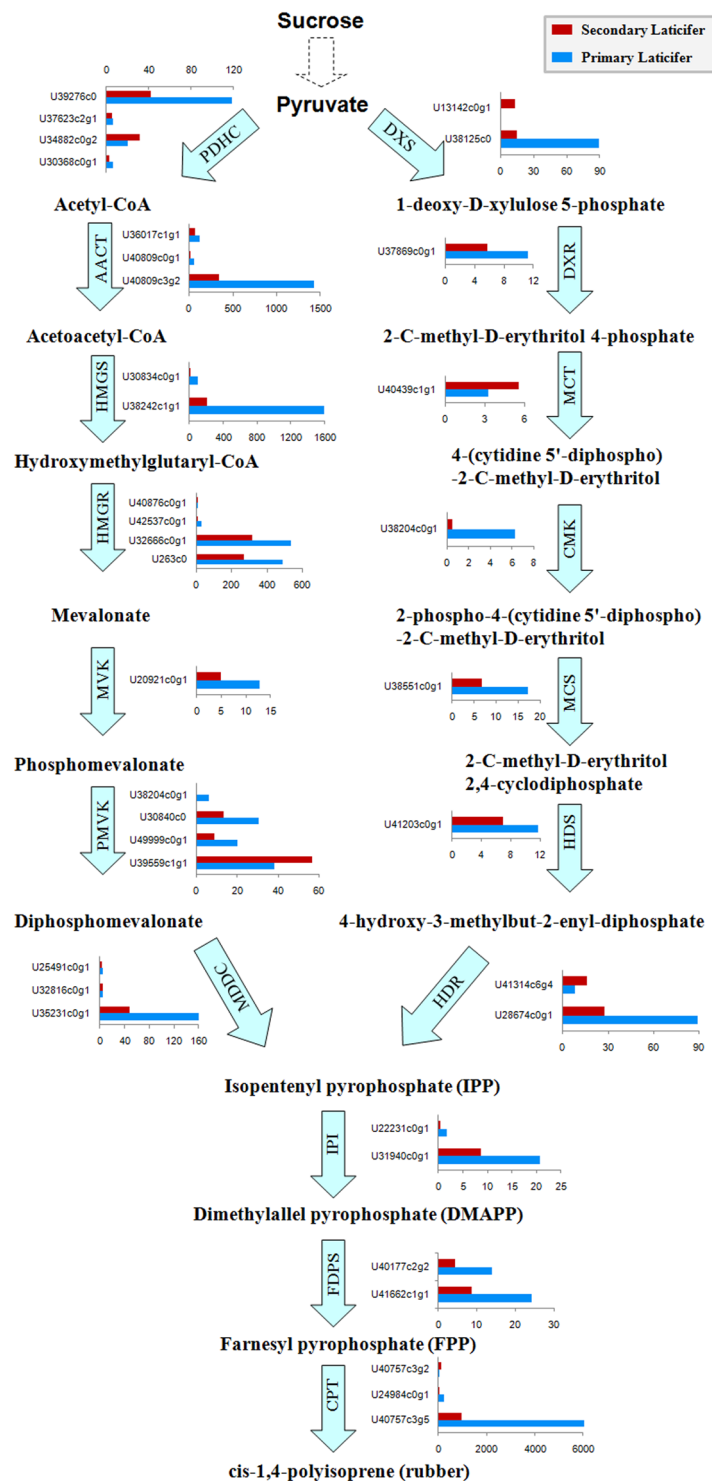


Figure 6. The rubber biosynthesis pathways and genes involved. The expression levels of each unigene in TPM are presented beside the enzymes.

When this method was used for morphological comparison between the primary and the secondary laticifer cells in this study, only the distribution patterns of the laticifer cells were found to be different. The primary laticifer cells were distributed at random among the parenchyma cells (Fig. 1b), whereas the secondary laticifer cells were distributed in rows or rings (Fig. 1d).

Isolated laticifers proved to be an ideal method to study the morphology and development of laticifers. This method was previously reported in 1987⁴⁷. We modified this method by inclusion of a fixation step using FAA solution before boiling and by staining the isolated laticifer networks using iodine bromide solution instead of Sudan solution, which greatly improved the quality of the images. Based on our observation, the secondary

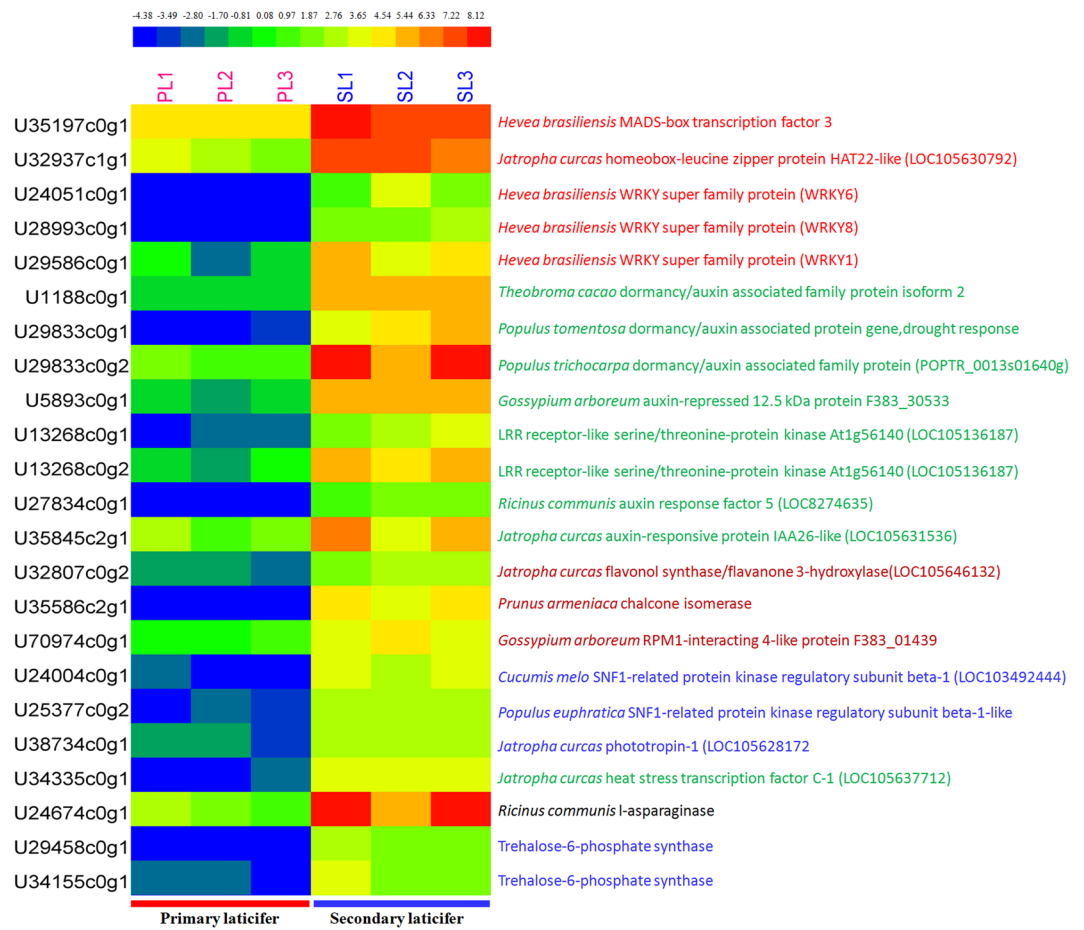


Figure 7. Heatmap of DEGs involved in abiotic stresses. The expression levels of DEGs in TPM were compiled with Excel 2007, normalized using a log₂ base method, and exported to the HemI toolkit¹²⁴. The figure was built using the default parameters. The expression levels are presented in different colors, and the values are defined in the scale bar. PL, the primary laticifers; SL, the secondary laticifers.

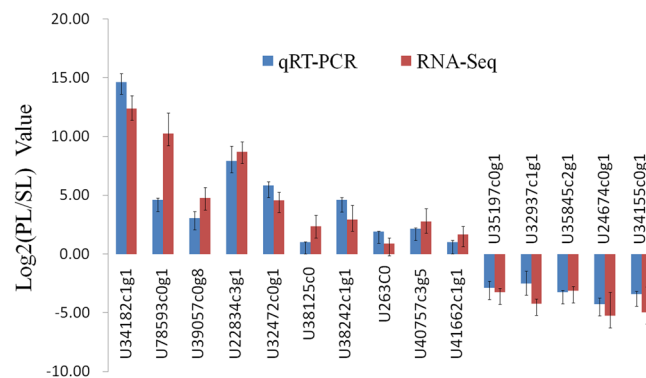


Figure 8. Quantitative RT-PCR validation of representative DEGs revealed by RNA-seq analysis.

laticifer cells had straight and smooth cell walls (Fig. 2h,i,j). The neighboring tubes were anastomosed by bridges, and each laticifer cell was joined to two or more cells of the neighboring tubes at different locations (Fig. 2h,i,j). These observations did not require expensive equipment, and the quality of these results were as good as previous observations gained with spectral confocal laser scanning microscopy⁴⁸. Moreover, the detailed laticifer structure of the primary laticifer network had never been revealed. We isolated the primary laticifer elements ranging from the meristem of young shoots to the mature region of branches and observed the sequential development and intrusive growth of the primary laticifers (Fig. 2a,b), as this growth was quite different from that of the secondary laticifer cells. The most impressive morphology of the primary laticifer vessels is the necklace-like structures (Fig. 2e) that are formed during intrusive growth. The neighboring “beads” then merged to form laticifer tubes

of larger diameter. The neighboring primary laticifer tubes were connected by bridges to form a laticifer network (Fig. 2f,g), which is similar to the secondary laticifer network.

Necklace-like morphology of the primary laticifers is facilitated by over-expression of cell wall process genes.

The rubber latex collected from rubber tree, either from the primary laticifers or from the secondary laticifers, is the cytoplasm of laticifer cells⁸ and contains the transcriptome of the laticifer cells. Therefore, the rubber latex provides a convenient material to study the transcriptome profiles of the single cell types. In order to collect the latex, however, the bark of the rubber trees was cut, and the neighboring cells of the laticifer cells were also broken, contributing to possible contamination of the latex. To reduce this potential contamination, the latex flow of the first 5 min for the secondary laticifers or the first droplet for the primary laticifers was discarded. To further eliminate contaminated RNA, a threshold cut-off TPM >1 was arbitrarily used to minimize false-positive gene expression data.

Through comparative analysis, we found that the primary and secondary laticifers exhibited distinct expression profiles. One of the most significant differences was that DEGs involved in cell wall processes were up-regulated in the primary laticifers (Fig. 4), corresponding to the necklace-like morphology of these cells. We identified eight pectinesterase genes that were highly up-regulated in the primary laticifers (Fig. 4). Pectinesterase is a ubiquitous cell wall-associated enzyme that facilitates pectin de-esterification and promotes pectin degradation especially during fruit ripening^{19,20}. Mutational disruption of the pectin methylesterase 3 (AtPME3) gene in *Arabidopsis thaliana* resulted in changes in pectin methylesterification status and caused hypersensitivity towards the specific interference of Zn⁺² with cell wall-controlled growth processes⁴⁹. Over-expression of a fungal pectin methylesterase gene in tobacco led to alterations in cell wall metabolism and a dwarf phenotype⁵⁰. The strong up-regulation of pectinesterase in the primary laticifers may play a major role in the intrusive growth and the formation of necklace-like structures of the primary laticifers (Fig. 2).

In addition to pectinesterase genes, DEGs related to plant-type cell wall construction were found to be highly up-regulated in the primary laticifers (Fig. 4). These genes include berberine bridge enzyme, class III peroxidase, alpha-expansin, RALF-like protein, subtilisin-like protease, alpha-glucosidase, and heparanase-like protein. Berberine bridge enzyme (BBE)-like enzymes has recently been demonstrated to play a role in plant cell wall metabolism via oxidation of monolignol⁵¹. *Arabidopsis* Class III peroxidase (AtPRX71) was shown to strengthen cell walls and restrict cell expansion during normal growth and in response to cell wall damage⁵². Alpha-expansin is a well-known cell wall component that plays a key role in “acid-growth” of plant cells⁵³. Rapid alkalization factor (RALF) is a secreted peptide that mediates a rapid alkalization of extracellular space by mediating a transient increase in the cytoplasmic Ca²⁺ concentration, leading to calcium-dependent signaling events and regulation of cell expansion^{54,55}. Disruption of the *kexB* gene that encodes a subtilisin-like processing protease in *Aspergillus oryzae* caused a decrease in cell wall alpha-1,3-glucan and substantial morphological defects⁵⁶. Furthermore, a subtilisin-like serine protease was found to be essential for mucilage release from *Arabidopsis* seed coats⁵⁷. Heparanase-like protein, an endoglycosidase, is a cell surface protein and an extracellular matrix-degrading enzyme that catalyzes the hydrolysis of heparan sulfate proteoglycans (HSPGs) into heparan sulfate side chains and core proteoglycans, and may have a role in cell growth regulation^{58–60}.

DEGs that were up-regulated in the primary laticifers also included genes related to lignin metabolic processes in the cell wall, and such genes included a laccase, a transaldolase, and three xylem serine protease genes. Laccase activity is important to cell wall reconstitution in regenerating protoplasts⁶¹, and downregulation of laccase caused alterations in phenolic metabolism and cell wall structure in *Populus trichocarpa*⁶². Additionally, knock-down of a laccase in *Populus deltoides* altered cell wall chemistry and increased sugar release⁶³. Transaldolase is an enzyme of the pentose phosphate pathway and plays an important role in lignin biosynthesis^{64,65} and biocontrol function⁶⁶. Differential expression of xylem serine protease genes has been shown to be one of the major causes of ruptured cell walls in the defective seed coats of a soybean mutant⁶⁷.

DEGs that were clustered in the cell size-regulation category encoded two metallothionein 3-like proteins, a WAT1-like protein, and a glucan endo-1, 3-beta- glucosidase. Metallothionein -like proteins, which are metal-binding proteins, function as detoxifier and are up-regulated in animal and plant cells upon exposure to heavy metals^{68–71}. However, they are also involved in fruit ripening of strawberries⁷², post-harvest senescence of *Alstroemeria* flowers⁷³, and somatic embryogenesis of white spruce⁷⁴, albeit via an unknown mechanism. In *Arabidopsis thaliana* WAT1 encodes a plant-specific, predicted integral membrane protein, and its expression is preferentially associated with vascular tissues, including developing xylem vessels and fibers⁷⁵. Mutation of WAT1 in *Arabidopsis* results in cell elongation defect⁷⁵. Glucan endo-1, 3-beta- glucosidase is an important component of plant cell walls⁷⁶ and plays a role in defense against fungal pathogens⁷⁷. It also plays a role in compression stress resistance, because lowering the amount of callose results in reduced cellular stiffness and increased viscoelasticity of pollen tubes⁷⁸. The up-regulation of glucan endo-1,3-beta-glucosidase in the primary laticifers suggest some similarities in the growth patterns of primary laticifers and pollen tubes.

Interestingly, three DEGs that were highly up-regulated in the primary laticifer cells were clustered in the categories of pollen tube guidance and regulation of pollen growth, and these genes were an annexin-like protein (U39057c0g8), a nucleoredoxin-like protein (U31194c0g1), and an early nodule-specific protein homolog (*Hev b 13*, U78593c0g1). Annexins interact with cell-membrane components that are relevant to the structural organization of the cell and to changes in the cell shape, intracellular signaling, growth control, and these proteins also act as atypical calcium channels^{23,24}. Annexins have been implicated in regulation of pollen tube and fiber growth in *Arabidopsis* and cotton^{21,22}. Nucleoredoxin functions as a redox-dependent negative regulator and/or a transcriptional regulator^{79–81}, and is critical for growth of pollen tubes in pistil of *Arabidopsis*⁸². The early nodule-specific protein homolog (*Hev b 13*) is an allergenic lipolytic esterase and is homologous to patatin⁸³, a potato (*Solanum tuberosum*) protein. Patatin is thought to be a storage protein that mainly localizes to the vacuole of the potato tube^{84,85}; however, it also has lipid acyl hydrolase activity⁸⁵. The patatin-like protein in rubber laticifers was not

localized to the vacuole⁸⁶, and exhibited lipid acyl-transferase and PLA2-like activity⁸⁷. As a result, this protein may catalyze the cleavage of fatty acids from membrane lipids and thus may function in the reconstruction of the laticifer membrane and/or defense against pests. Moreover, a patatin-like protein was found to be critical to the programmed degeneration of the *Arabidopsis* sporophytic tapetum to support pollen development⁸⁸. These data further suggest that the development and growth of the primary laticifer cells may have some similarities to pollen grains and pollen tubes.

Two DEGs that were clustered in the category of cell wall macromolecule catabolic processes included a lysin motif (LysM) domain receptor-like kinase 3 (Lyk3, U28972c0g1) and a wall-associated receptor kinase (U38208c0g2). Lyk3 may recognize microbe-derived N-acetylglucosamine (NAG)-containing ligands and regulate the cross talk between immunity and abscisic acid responses in *Arabidopsis*⁸⁹. Furthermore, this protein was found to be an entry receptor in rhizobial nodulation factor signaling in *Medicago*⁹⁰, and its localization and dynamics were altered in response to symbiotic bacteria⁹¹. Wall-associated kinase (WAK) and WAK-like kinase (WAKL) constitute a family of receptor-like kinase genes that encode transmembrane proteins⁹², and some of the members were co-expressed with pathogen defense related genes^{93,94}, whereas others were required for cell elongation and plant development⁹².

Taken together, these data demonstrate a considerable number of DEGs that are related to cell wall modification and cell development were up-regulated in the primary laticifers, resulting in the active intrusive growth of the primary laticifer cells and the formation of necklace-like morphology.

Up-regulation of lytic enzymes in the primary laticifers suggests a role for defense against biotic stresses.

We have demonstrated that many genes that function in defense against biotic stress, especially genes that encode lytic enzymes, are highly up-regulated in the primary laticifers. These genes include (S)-hydroxynitrile lyase, beta-cyanoalanine synthase, polyphenol oxidase, chitinase, and glucanase (Fig. 5). Among these genes, (S)-hydroxynitrile lyase genes (HNL) were the most significant DEGs. HNL catalyzes the hydrolysis of (S)-hydroxynitriles and releases toxic cyanide, which serves as a defense mechanism against herbivores and microbial attack in plants²⁹. The (S)-hydroxynitrile lyase gene was first cloned by Hasslacher and colleagues from the leaves of *Hevea brasiliensis*³⁰ and was over-expressed heterologously in *Escherichia coli* and *Saccharomyces cerevisiae*⁹⁵. Our report is the first to demonstrate that the (S)-hydroxynitrile lyase gene was highly up-regulated in the primary laticifer cells than in the secondary laticifer cells. Protease inhibitors are known as defense proteins and have been over-expressed in crops for herbivore pest control⁹⁶. Chitinases have been identified in the laticifers of numerous latex-containing species, including monocotyledons, dicotyledons, and a gymnosperm^{97–100}. These enzymes were also identified at high levels in the laticifer cells of rubber tree¹⁰¹. Microbial chitinases have been shown to exhibit antifungal activity and used for biological control against plant fungal diseases^{102–105}. Chitinases of insect origin also exhibit toxic effects on other insects upon oral ingestion^{106,107}. In latex-containing plants, jasmonic acid, a plant hormone that is involved in signal transduction of plant responses to herbivory, was proven to induce expression of chitinases in the latex of *Ficus carica*¹⁰⁸, and expression of chitinases in the latex of *C. papaya* was found to be induced by wounding¹⁰⁹. Furthermore, a poplar chitinase was over-expressed in tomato and inhibited the development of the Colorado potato beetle¹¹⁰. These results suggest that chitinases in latex may play a defensive role. Because chitin is the major component of the cell walls of fungi and some insects, it is reasonable to speculate that chitinases in the laticifer cells of rubber trees may protect the plants from fungal infection and insect attacks.

The laticifer cells of the rubber tree are dedicated primarily to the biosynthesis of rubber (*cis*-1,4-polyisoprene); thus, the most highly expressed genes in the laticifer cells are likely to be genes involved in the biosynthesis of rubber. Indeed, gene transcripts encoding enzymes involved in rubber biosynthesis are 20– to 100–fold higher in laticifers than in leaves¹¹¹; however, several putative defense genes, including chitinases, pathogenesis-related proteins, phenylalanine ammonia-lyase, chalcone synthase, chalcone isomerase, and 5-enolpyruvylshikimate 3-phosphate synthase, are also expressed at 10– to 50–fold higher levels in laticifers than in leaves¹¹¹. Chitinases/lysozymes are the most abundant proteins in the latex, are localized primarily in the lutoid, and account for approximately 20% of the total soluble protein of the latex¹⁰¹. The above findings are all based on analysis of the secondary laticifers. Here, we compared the transcriptional profiles of the primary and the secondary laticifer cells and revealed that the expression levels of (S)-hydroxynitrile lyases, chitinases, glucanases, and protease inhibitors are up-regulated in the primary laticifer cells. Confirmation of these findings via qRT-PCR supports this comparison and suggests that the primary laticifer cells and/or the young tissues are more adequately prepared to defend against attacks by herbivorous animals and pathogens than the secondary laticifers.

Up-regulation of DEGs in the secondary laticifers suggests defense against abiotic stresses.

We have demonstrated that the secondary laticifer cells of untapped rubber trees display features of dormancy and abiotic stress resistance. DEGs that were up-regulated in the secondary laticifers include transcription factors and signal receptors of brassinosteroid, karrikin, sucrose, and auxin (Fig. 7), which are related to dormancy. This differential expression may have resulted in the down-regulation of DEGs involved in rubber biosynthesis (Fig. 6). The obviously abiotic stress-related DEGs that were up-regulated in the secondary laticifers include trehalose-phosphate synthase genes, heat stress-responsive transcription factor C-1 genes, and an asparaginase gene (Fig. 7). Trehalose-phosphate synthase genes have been reported to enhance drought resistance^{42,43}, while the heat stress-responsive transcription factor C-1 in *Arabidopsis* and rice regulates the expression of heat shock proteins^{44,45}. In addition, an asparaginase (GmASP1) in soybean is induced by cold stress⁴⁶. Therefore, the rubber tree asparaginase homolog is potentially related to cold stress. Taken together, these findings indicate that the secondary laticifer cells are more adequately prepared to defend against abiotic stresses than the primary laticifers.

Rubber biosynthesis is more active in the primary laticifers of the untapped rubber trees. The latex tapped from the secondary laticifer cells of the trunk of the rubber trees (>6 years old) were the major source of natural rubber, however, the primary laticifer cells were actually more active in rubber biosynthesis in the untapped rubber trees (Fig. 6). This observation does not mean that the secondary laticifer cells are not as productive as the primary laticifer cells. The down-regulation of the rubber biosynthesis genes in the secondary laticifer cells (Fig. 6), however, may be explained by the dormancy of the secondary laticifer cells induced by dormancy-related genes (Fig. 7), since the secondary laticifer tubes may be full of rubber particles in trees that have not been tapped for 6 years. Previous evidence has suggested that tapping stimulates rubber biosynthesis in the secondary laticifer cells^{41,112}.

In conclusion, the primary and the secondary laticifer cells are morphologically and functionally distinct. Genes involved in cell wall modification were highly up-regulated in the primary laticifers, and correspond to the necklace-like morphology of the primary laticifer tubes. By contrast, the cell walls of the secondary laticifer cells were relatively smooth and straight. The primary and the secondary laticifer cells are also functionally different. Genes involved in defense against biotic stresses were highly up-regulated in the primary laticifer cells, whereas genes involved in abiotic stresses and dormancy were highly up-regulated in the secondary laticifer cells. These findings suggest that the primary laticifer cells are more adequately prepared to defend against biotic stresses such as insects and pathogens, while the secondary laticifer cells are more adequately prepared to defend against abiotic stresses. Interestingly, genes involved in rubber biosynthesis were highly up-regulated in the primary laticifers compared with those in the secondary laticifer cells. These observations could be explained by feedback inhibition in the secondary laticifer tubes, because the secondary laticifer cells in trees that have not been tapped for 7 years may be full of rubber particles. Taken together, these findings indicate that the two types of laticifers are morphologically and functionally distinct.

Methods

Histochemical analysis of the primary and the secondary laticifers. Rubber trees (*Hevea brasiliensis* Mull. Arg.) used in this study were grafted plants of clone RY7-33-97 using the seedlings of RY7-33-97 as rootstock. The plants were grown on the experimental farm of the Chinese Academy of Tropical Agricultural Sciences in Danzhou City, Hainan Province for 7 years without tapping. Histochemical observation of cross-sections of the bark of the tree trunks and young branches was performed as previously described¹¹³ with a few modifications. The bark samples of the tree trunks and epicormic young branches as shown in Fig. 1 were excised and fixed in FAA solution (5 mL formalin, 5 mL glacial acetic acid, 90 mL 70% ethanol) for 3 d. After dehydration in an ethanol/*n*-butyl alcohol series, the samples were treated with an iodine and bromine solution (5 g iodine, 0.4 mL bromine, and 100 mL glacial acetic acid)¹⁰ for 36 h at 60 °C. The samples were washed with glacial acetic acid, dehydrated in an *n*-butyl alcohol series, and embedded in paraffin. Sections of 10 µm were prepared with a rotary microtome (LEICA RM2245, Wetzlar, Germany), dewaxed in xylene, and stained with fast green solution (5 g of fast green in 100 ml of 95% ethanol). The sections were viewed and photographed with a light microscope (Axioskop 40, Zeiss, Oberkochen, Germany).

To study the three-dimensional morphology of the laticifer networks, the primary and the secondary laticifer networks were isolated using a previously described method⁴⁷ with a few modifications. The bark samples of the tree trunks and segments of the young branches from three 7-year-old untapped rubber trees as shown in Fig. 1 were fixed in FAA solution for 24 h, boiled in 10% KOH for 20 min as previously described⁴⁷, and then rinsed in running water for 2 h. The laticifer networks were dissected from the samples under a dissecting microscope by removing the peridermal layers and the parenchyma cells surrounding the laticifer cells with a pair of forceps and a dissecting needle. The laticifer cells were then stained with iodine bromide solution¹¹⁴ and observed and photographed with a light microscope.

Latex collection and total RNA extraction. A total of 18 healthy untapped 7-year-old rubber trees (clone RY7-33-97) were randomly selected, in which nine were used for collecting primary latex and the other nine were used for collecting secondary latex. Three independent latex replicates were collected from each of the primary and the secondary laticifer cells during different seasons (July 2014, October 2014, and April 2015) to minimize the possible influence of seasonal changes in the transcriptome profiles, and each sample contained the latex of the primary or the secondary laticifer cells of three trees. The latex of the secondary laticifer cells was collected by tapping the bark of the trunk 1 m above the ground (Fig. 1a). To reduce contamination by non-laticifer RNAs from neighboring cells, the latex flow of the first 5 min was discarded, and the remaining latex was collected in 50-mL centrifuge tubes on ice. To collect latex from the primary laticifer cells, the barks of the epicormic shoots (Fig. 2b) were cut with a sharp scalpel. To reduce contamination by non-laticifer RNAs from neighboring cells, the first drop of latex was discarded, and the remaining latex was collected in 1.5-mL centrifuge tubes and stored on ice. Total RNA was extracted as previously described¹¹⁵. The quality of the total RNA was evaluated using a 2100 Bioanalyzer (Agilent Technologies, Santa Clara, CA, USA).

Construction of cDNA library and sequencing. Poly(A) mRNA was enriched from total RNA using magnetic beads with Oligo (dT) (Dynabeads, Invitrogen, Carlsbad, CA, USA). The enriched mRNA was randomly broken into short fragments and reverse transcribed to cDNA using the Superscript III First-Strand Synthesis System (Invitrogen). Double-strand (ds) cDNA was synthesized using DNA polymerase I and RNase H (TaKaRa, Dalian, China), and purified with an Agencourt AMPure XP Kit (Beckman Coulter, Beijing, China). Adapters were then added to the two ends of the ds cDNA, and molecules were then amplified by PCR to construct the sample library. The quality of the libraries was evaluated by Agilent 2100 Bioanalyzer and ABI StepOnePlus Real-Time PCR System. The libraries of replicate I were sequenced using Illumina HiSeq™ 2000 with an average

read length of 90 nt (BGI, Shenzhen, China). Replicates II and III were sequenced using HiSeq2500 with an average read length of 100 nt (Biomarker, Beijing, China).

De novo sequence assembly, annotation, and classification. Raw reads that had more than 10% of bases with low-quality scores ($Q < 20$) and those that still contained adaptors and unknown nucleotides of more than 5% were filtered with Filter_fq software. *De novo* assembly of the clean reads was performed using Trinity Version 2.1.1¹⁶, according to the recommended protocol. In addition, bowtie V1.1.2¹⁷, a plug-in program in the Trinity software, was used.

The unigenes were annotated by homology searches against the public databases, including the non-redundant NCBI peptide database (NR, <http://www.ncbi.nlm.nih.gov>), Swiss-Prot (<http://www.expasy.ch/sprot/>), the Kyoto Encyclopedia of Genes and Genomes (KEGG, <http://www.genome.jp/kegg/>), and the Cluster of Orthologous Groups (COG, <http://www.ncbi.nlm.nih.gov>) using the BLASTX software¹⁶ with a cut-off value of $1E-5$. The unigenes were also screened against the NCBI nucleotide database (NT) using the BLASTN program. The best alignment results were accepted for annotation of the unigenes.

To perform functional classification of the unigenes, GO annotation was carried out using the Blast2GO program (<http://www.geneontology.org>) based on the molecular function, biological process, and cellular component.

Mapping and detection of DEGs. The eXpress method¹¹⁷ was used to estimate gene abundance. The expression values of reads were normalized using the trimmed mean of M values (TMM) method^{118,119}. To minimize the detection of false positives in gene expression of the laticifer cells, a threshold cut-off of TPM > 1 was arbitrarily used to identify genes that were expressed in at least one sample. To identify DEGs, the raw counts were examined with EdgeR using standard parameters¹⁸, and an adjusted p -value cut-off ≤ 0.001 was used for FDR.

Functional enrichment analysis for DEGs. Before GO enrichment analysis, a GO annotation list of each unigene was generated using the Blast2GO program, and genes were grouped into categories based on biological properties according to the data of “go_201603-termdb-data.gz” in the GO database. A GO-Seq package¹²⁰ was utilized to analyze the enriched and depleted GO categories for genes that were either up-regulated or down-regulated in the pair-wise DE analysis, a p -value cut-off of 0.05 was used.

Additionally, to gain insight into the pathways altered between the primary and the secondary laticifer cells, DEGs were annotated and imported to MapMan¹²¹ for visualization.

Validation of representative DEGs by qRT-PCR. Real-time PCR was used to validate transcriptome analysis results in accordance to MIQE guideline¹²². We selected fifteen genes with significant differential expression levels and important biological functions for real-time PCR confirmation. The stable reference genes of a ubiquitin-protein ligase (HQ323249), eIF1Aa (HQ268022), and YLS8 (HQ323250)¹²³ were used to normalize the expression levels. The primers (Supplementary Table S5) were designed by Primer Premier 5.0 software and were verified by sequencing their amplified fragments. Rubber latex of the primary and the secondary laticifers were collected as described above with three biological replicates. Total RNA was extracted as previously described¹¹⁵. The quality of the total RNA was evaluated using a 2100 Bioanalyzer (Agilent Technologies, Santa Clara, CA, USA). The RNA integrity number (RIN) values of the RNA samples are provided in Supplementary Table S6. First-strand cDNA was synthesized using the Revertaid™ First Strand cDNA Synthesis Kit (Fermentas, Canada). The efficiency of each primer pair was estimated as ranging from 1.89 and 1.99. Then, qRT-PCR was performed with the SYBR® Premix Ex Taq™ II Kit (Takara, Japan) according to the manufacturer's protocol. A 20- μ l reaction mix composed of 10 μ l SYBR® Premix Ex Taq II (2x), 0.4 μ l ROX Reference Dye (50x), 100 ng of template cDNA, 0.8 μ l PCR forward primer (10 μ M), and 0.8 μ l PCR reverse primer (10 μ M) was used. The reaction was performed in a Rotor Gene6000 (Corbett Research, Sydney, Australia) using the following parameters: pre-denaturation at 95 °C for 30 s, followed by 40 cycles of denaturation at 95 °C for 5 s, annealing at 58 °C for 30 s, and elongation at 72 °C for 30 s. The experiments were performed with three biological replicates and three technique replicates. The relative expression levels of the target genes were determined using the $2^{-\Delta\Delta Ct}$ method¹²⁵. The significance of the correlation between the RNA-Seq and qRT-PCR results was analyzed using IBM SPSS Statistics Version 24, and the correlation curves were created with Excel 2007 (Microsoft Inc., USA).

References

- Mooibroek, H. & Cornish, K. Alternative sources of natural rubber. *Appl. Microbiol. Biot* **53**, 355–365, doi:10.1007/s002530051627 (2000).
- da Costa, B. M., Keasling, J. D. & Cornish, K. Regulation of rubber biosynthetic rate and molecular weight in *Hevea brasiliensis* by metal cofactor. *Biomacromolecules* **6**, 279–289, doi:10.1021/bm049606w (2005).
- Parth, M. N., A. & Lederer, K. Distribution of molar mass and branching index of natural rubber from *Hevea brasiliensis* trees of different age by size exclusion chromatography coupled with online viscometry. *Macromol. Symp.* **181**, 447–456, doi:10.1002/(ISSN)1521-3900 (2002).
- Bonfils, F. & Char, C. In *Encyclopedia of Chromatography* (Taylor & Francis, 2011).
- Davis, W. The rubber industry's biological nightmare. *Fortune* **4**, 86–95 (1997).
- Threadingham, D., Obrecht, W., Wieder, W., Wachholz, G. & Engehasen, R. *Rubber, 3. Synthetic Rubbers, Introduction and Overview* (Ullmann's Encyclopedia of Industrial Chemistry, 2011).
- Evert, R. F. In *Esau's Plant Anatomy* (ed. R.F. Evert) 473–501 (John Wiley & Sons, Inc., 2006).
- Hagel, J. M., Yeung, E. C. & Facchini, P. J. Got milk? The secret life of laticifers. *Trends Plant Sci.* **13**, 631–639, doi:10.1016/j.tplants.2008.09.005 (2008).
- Verheyne, W. In *Land Use, Land Cover and Soil Sciences. Encyclopedia of Life Support Systems (EOLSS) Vol.* <http://www.eolss.net> (ed. W. Verheyne) (UNESCO-EOLSS Publishers, 2010).
- Hao, B. Z. & Wu, J. L. Laticifer differentiation in *Hevea brasiliensis*: induction by exogenous jasmonic acid and linolenic acid. *Ann. Bot* **85**, 37–43, doi:10.1006/anbo.1999.0995 (2000).

11. d'Auzac, J., Jacob, J. L. & Chrestin, H. *Physiology of rubber tree latex* (CRC Press, Inc., 1989).
12. Zeng, X., Hu, Y., Huang, H. & Fang, J. Evaluation of the major characteristics of IRRDB 1981 rubber tree germplasm planted in 1987. *Chinese J. Trop. Crops* **27**, 34–37 (2006).
13. Yu, J. H., Zeng, X., Yang, S. G., Huang, H. S. & Tian, W. M. Relationship between rate of laticifer differentiation, number of laticifer rows and rubber yield among 1981 IRRDB germplasm collections of *Hevea brasiliensis*. *J. Rubb. Res* **11**, 43–51 (2008).
14. Zhou, Z. *et al.* Relationship between Hevea latex vessel system and yield prediction at nursery stage. *Chinese J. Trop. Crops* **5**, 29–36 (1984).
15. Zeng, X., Hu, Y., Fang, J. & Huang, H. Main characteristics evaluation of wild Hevea germplasm 1981 IRRDB. *J. Plant Genet. Resour* **8**, 35–40 (2007).
16. Grabherr, M. G. *et al.* Trinity: reconstructing a full-length transcriptome without a genome from RNA-Seq data. *Nat. Biotechnol.* **29**, 644–652 (2011).
17. Haas, B. J. *et al.* De novo transcript sequence reconstruction from RNA-Seq: reference generation and analysis with Trinity. *Nat. Protoc.* **8**, doi:10.1038/nprot.2013.1084 (2013).
18. Robinson, M. D., McCarthy, D. J. & Smyth, G. K. edgeR: a Bioconductor package for differential expression analysis of digital gene expression data. *Bioinformatics* **26**, 139–140, doi:10.1093/bioinformatics/btp616 (2010).
19. Carpita, N. C., Campbell, M., Tierney, M., Brummell, D. & Harpster, M. In *Plant Cell Walls* 311–340 (Springer Netherlands, 2001).
20. Micheli, F. Pectin methylesterases: cell wall enzymes with important roles in plant physiology. *Trends Plant Sci.* **6**, 414–419, doi:10.1016/S1360-1385(01)02045-3 (2001).
21. Wang, L. K., Niu, X. W., Lv, Y. H., Zhang, T. Z. & Guo, W. Z. Molecular cloning and localization of a novel cotton annexin gene expressed preferentially during fiber development. *Mol. Bio. Rep* **37**, 3327–3334, doi:10.1007/s11033-009-9919-2 (2010).
22. Zhu, J. *et al.* Annexin5 plays a vital role in Arabidopsis pollen development via Ca²⁺-dependent membrane trafficking. *PLoS One* **9**, e102407, doi:10.1371/journal.pone.0102407 (2014).
23. Moss, S. E. & Morgan, R. O. The annexins. *Genome Biol.* **5**, 219–219, doi:10.1186/gb-2004-5-4-219 (2004).
24. Franklin-Tong, V. E. Signaling and the Modulation of Pollen Tube Growth. *The Plant Cell* **11**, 727–738, doi:10.1105/tpc.11.4.727 (1999).
25. Fudali, S. *et al.* Expansins are among plant cell wall modifying agents specifically expressed during development of nematode-induced syncytia. *Plant Signal. Behav* **3**, 969–971, doi:10.4161/psb.6169 (2008).
26. Fudali, S. *et al.* Two tomato alpha-expansins show distinct spatial and temporal expression patterns during development of nematode-induced syncytia. *Physiol. Plant* **132**, 370–383, doi:10.1111/ppl.2008.132.issue-3 (2008).
27. Wieczorek, K. *et al.* Expansins are involved in the formation of nematode-induced syncytia in roots of Arabidopsis thaliana. *Plant J* **48**, 98–112, doi:10.1111/tj.2006.48.issue-1 (2006).
28. Wieczorek, K. & Grundle, F. M. Expanding nematode-induced syncytia: the role of expansins. *Plant Signal. Behav* **1**, 223–224, doi:10.4161/psb.1.5.3426 (2006).
29. Poulton, J. E. Cyanogenesis in Plants. *Plant Physiol.* **94**, 401–405, doi:10.1104/pp.94.2.401 (1990).
30. Hasslacher, M. *et al.* Molecular cloning of the full-length cDNA of (S)-hydroxynitrile lyase from *Hevea brasiliensis*. Functional expression in *Escherichia coli* and *Saccharomyces cerevisiae* and identification of an active site residue. *J. Bio. Chem.* **271**, 5884–5891, doi:10.1074/jbc.271.10.5884 (1996).
31. Kongsawadworakul, P. *et al.* The leaf, inner bark and latex cyanide potential of *Hevea brasiliensis*: evidence for involvement of cyanogenic glucosides in rubber yield. *Phytochemistry* **70**, 730–739, doi:10.1016/j.phytochem.2009.03.020 (2009).
32. Constabel, C. P. & Barbehenn, R. In *Induced Plant Resistance to Herbivory* (ed. A. Schaller) (Springer Science+Business Media B. V., 2008).
33. Bokma, E. *et al.* Determination of cDNA and genomic DNA sequences of hevamine, a chitinase from the rubber tree *Hevea brasiliensis*. *Plant Physiol. Biochem.* **39**, 367–376, doi:10.1016/S0981-9428(01)01247-5 (2001).
34. Lusso, M. & Kuc, J. The effect of sense and antisense expression of the PR-N gene for β -1,3-glucanase on disease resistance of tobacco to fungi and viruses. *Physiol. Mol. Plant Path.* **49**, 267–283, doi:10.1006/pmpp.1996.0054 (1996).
35. Kuc, J. Phytoalexins, stress metabolism, and disease resistance in plants. *Annu. Rev. Phytopathol.* **33**, 275–297, doi:10.1146/annurev.py.33.090195.001423 (1995).
36. Archer, B. L., Audley, B. G., Cockbain, E. G. & McSweeney, G. P. The biosynthesis of rubber. Incorporation of mevalonate and isopentenyl pyrophosphate into rubber by *Hevea brasiliensis*-latex fractions. *Biochem. J.* **89**, 565–574, doi:10.1042/bj0890565 (1963).
37. Chye, M. L., Tan, C. T. & Chua, N. H. Three genes encode 3-hydroxy-3-methylglutaryl-coenzyme A reductase in *Hevea brasiliensis*: hmg1 and hmg3 are differentially expressed. *Plant Mol. Biol.* **19**, 473–484, doi:10.1007/BF00023395 (1992).
38. Chow, K. S. *et al.* Metabolic routes affecting rubber biosynthesis in *Hevea brasiliensis* latex. *J. Exp. Bot* **63**, 1863–1871, doi:10.1093/jxb/err363 (2012).
39. Asawatreratanakul, K. *et al.* Molecular cloning, expression and characterization of cDNA encoding cis-prenyltransferases from *Hevea brasiliensis*. A key factor participating in natural rubber biosynthesis. *Eur. J. Biochem* **270**, 4671–4680, doi:10.1046/j.1432-1033.2003.03863.x (2003).
40. Koyama, T. Molecular analysis of prenyl chain elongating enzymes. *Biosci. Biotech Bioch* **63**, 1671–1676, doi:10.1271/bbb.63.1671 (1999).
41. Chao, J., Chen, Y., Wu, S. & Tian, W. M. Comparative transcriptome analysis of latex from rubber tree clone CATAS8-79 and PR107 reveals new cues for the regulation of latex regeneration and duration of latex flow. *BMC Plant Biol* **15**, 104, doi:10.1186/s12870-015-0488-3 (2015).
42. Avonce, N. *et al.* The Arabidopsis trehalose-6-P synthase AtTPS1 gene is a regulator of glucose, abscisic acid, and stress signaling. *Plant Physiol.* **136**, 3649–3659, doi:10.1104/pp.104.052084 (2004).
43. Karim, S. *et al.* Improved drought tolerance without undesired side effects in transgenic plants producing trehalose. *Plant Mol. Biol.* **64**, 371–386, doi:10.1007/s11103-007-9159-6 (2007).
44. Guo, J. *et al.* Genome-wide analysis of heat shock transcription factor families in rice and Arabidopsis. *J. Genet. Genomics. Journal of genetics and genomics = Yi chuan xue bao* **35**, 105–118, doi:10.1016/S1673-8527(08)60016-8 (2008).
45. Nover, L. *et al.* Arabidopsis and the heat stress transcription factor world: how many heat stress transcription factors do we need? *Cell Stress Chaperon* **6**, 177–189, doi:10.1379/1466-1268(2001)006<0177:AATHST>2.0.CO;2 (2001).
46. Cho, C. W. *et al.* Molecular characterization of the soybean L-asparaginase gene induced by low temperature stress. *Mol. Cells* **23**, 280–286 (2007).
47. Zhao, X. Q. The significance of the structure of laticifer with relation to the exudation of latex in *Hevea brasiliensis*. *J. Nat. Rubb. Res* **2**, 94–98 (1987).
48. Sando, T. *et al.* Histochemical study of detailed laticifer structure and rubber biosynthesis-related protein localization in *Hevea brasiliensis* using spectral confocal laser scanning microscopy. *Planta* **230**, 215–225, doi:10.1007/s00425-009-0936-0 (2009).
49. Weber, M. *et al.* A mutation in the Arabidopsis thaliana cell wall biosynthesis gene pectin methylesterase 3 as well as its aberrant expression cause hypersensitivity specifically to Zn. *Plant J.* **76**, 151–164, doi:10.1111/tj.12279 (2013).
50. Hasunuma, T., Fukusaki, E. & Kobayashi, A. Expression of fungal pectin methylesterase in transgenic tobacco leads to alteration in cell wall metabolism and a dwarf phenotype. *J. Biotechnol.* **111**, 241–251, doi:10.1016/j.jbiotec.2004.04.015 (2004).

51. Daniel, B. *et al.* Oxidation of monolignols by members of the berberine bridge enzyme family suggests a role in plant cell wall metabolism. *J. Biol. Chem.* **290**, 18770–18781, doi:10.1074/jbc.M115.659631 (2015).
52. Raggi, S. *et al.* The Arabidopsis Class III peroxidase AtPRX71 negatively regulates growth under physiological conditions and in response to cell wall damage. *Plant Physiol.* **169**, 2513–2525, doi:10.1104/pp.15.01464 (2015).
53. Durachko, D. M. & Cosgrove, D. J. Measuring plant cell wall extension (creep) induced by acidic pH and by alpha-expansin. *J. Vis. Exp.* **1263**, doi:10.3791/1263 (2009).
54. Haruta, M., Sabat, G., Stecker, K., Minkoff, B. B. & Sussman, M. R. A peptide hormone and its receptor protein kinase regulate plant cell expansion. *Science* **343**, 408–411, doi:10.1126/science.1244454 (2014).
55. Stes, E., Gevaert, K. & De Smet, I. Phosphoproteomics-based peptide ligand-receptor kinase pairing. Commentary on: “A peptide hormone and its receptor protein kinase regulate plant cell expansion”. *Front. Plant Sci.* **6**, 224, doi:10.3389/fpls.2015.00224 (2015).
56. Mizutani, O. *et al.* Substantial decrease in cell wall alpha-1,3-glucan caused by disruption of the kexB gene encoding a subtilisin-like processing protease in *Aspergillus oryzae*. *Biosci. Biotech. Biochem.* 1–11 (2016).
57. Rautengarten, C. *et al.* A subtilisin-like serine protease essential for mucilage release from Arabidopsis seed coats. *Plant J.* **54**, 466–480, doi:10.1111/j.1365-313X.2008.03437.x (2008).
58. Sivaram, P., Obunike, J. C. & Goldberg, I. J. Lysolecithin-induced alteration of subendothelial heparan sulfate proteoglycans increases monocyte binding to matrix. *J. Biol. Chem.* **270**, 29760–29765, doi:10.1074/jbc.270.50.29760 (1995).
59. Pillarisetti, S., Paka, L., Obunike, J. C., Berglund, L. & Goldberg, I. J. Subendothelial retention of lipoprotein (a). Evidence that reduced heparan sulfate promotes lipoprotein binding to subendothelial matrix. *J. Clin. Invest.* **100**, 867–874, doi:10.1172/JCI119602 (1997).
60. Chandrasekar, B. *et al.* Broad-range glycosidase activity profiling. *Mol. Cell. Proteomics* **13**, 2787–2800, doi:10.1074/mcp.O114.041616 (2014).
61. De Marco, A. & Roubelakis-Angelakis, K. A. Laccase activity could contribute to cell-wall reconstitution in regenerating protoplasts. *Phytochemistry* **46**, 421–425, doi:10.1016/S0031-9422(97)00301-4 (1997).
62. Ranocha, P. *et al.* Laccase down-regulation causes alterations in phenolic metabolism and cell wall structure in poplar. *Plant Physiol.* **129**, 145–155, doi:10.1104/pp.010988 (2002).
63. Bryan, A. C. *et al.* Knockdown of a laccase in *Populus deltoides* confers altered cell wall chemistry and increased sugar release. *Plant Biotechnol. J.* **14**, 2010–2020, doi:10.1111/pbi.12560 (2016).
64. Moehs, C. P., Allen, P. V., Friedman, M. & Belknap, W. R. Cloning and expression of transaldolase from potato. *Plant Mol. Biol.* **32**, 447–452, doi:10.1007/BF00019096 (1996).
65. Yang, Z. *et al.* Ancient horizontal transfer of transaldolase-like protein gene and its role in plant vascular development. *New Phytol.* **206**, 807–816, doi:10.1111/nph.13183 (2015).
66. Liu, J. Y., Li, S. D. & Sun, M. H. Transaldolase gene Tal67 enhances the biocontrol activity of *Clonostachys rosea* 67-1 against *Sclerotinia sclerotiorum*. *Biochem. Biophys. Res. Commun.* **474**, 503–508, doi:10.1016/j.bbrc.2016.04.133 (2016).
67. Kour, A., Boone, A. M. & Vodkin, L. O. RNA-Seq profiling of a defective seed coat mutation in Glycine max reveals differential expression of proline-rich and other cell wall protein transcripts. *PLoS One* **9**, e96342, doi:10.1371/journal.pone.0096342 (2014).
68. Ohi, S., Cardenosa, G., Pine, R. & Huang, P. C. Cadmium-induced accumulation of metallothionein messenger RNA in rat liver. *J. Biol. Chem.* **256**, 2180–2184 (1981).
69. Auguy, F. *et al.* Transcriptome changes in *Hirschfeldia incana* in response to lead exposure. *Front. Plant Sci.* **6**, 1231, doi:10.3389/fpls.2015.01231 (2015).
70. Banni, M. *et al.* Metallothionein gene expression in liver of rats exposed to cadmium and supplemented with zinc and selenium. *Arch. Environ. Contam. Toxicol.* **59**, 513–519, doi:10.1007/s00244-010-9494-5 (2010).
71. Hall, J. L. Cellular mechanisms for heavy metal detoxification and tolerance. *J. Exp. Bot.* **53**, 1–11, doi:10.1093/jxb/53.366.1 (2002).
72. Nam, Y. W. *et al.* Isolation and characterization of mRNAs differentially expressed during ripening of wild strawberry (*Fragaria vesca* L.) fruits. *Plant Mol. Biol.* **39**, 629–636, doi:10.1023/A:1006179928312 (1999).
73. Breeze, E. *et al.* Gene expression patterns to define stages of post-harvest senescence in *Alstroemeria petals*. *Plant Biotechnol. J.* **2**, 155–168, doi:10.1111/pbi.2004.2.issue-2 (2004).
74. Dong, J. Z. & Dunstan, D. I. Expression of abundant mRNAs during somatic embryogenesis of white spruce [*Picea glauca* (Moench) Voss]. *Planta* **199**, 459–466 (1996).
75. Ranocha, P. *et al.* Walls are thin 1 (WAT1), an Arabidopsis homolog of *Medicago truncatula* NODULIN21, is a tonoplast-localized protein required for secondary wall formation in fibers. *Plant J.* **63**, 469–483, doi:10.1111/tpj.2010.63.issue-3 (2010).
76. Uzal, E. N. *et al.* Analysis of the soluble cell wall proteome of gymnosperms. *J. Plant Physiol.* **166**, 831–843, doi:10.1016/j.jplph.2008.11.009 (2009).
77. Yeoh, K. A., Othman, A., Meon, S., Abdullah, F. & Ho, C. L. Sequence analysis and gene expression of putative exo- and endoglucanases from oil palm (*Elaeis guineensis*) during fungal infection. *J. Plant Physiol.* **169**, 1565–1570, doi:10.1016/j.jplph.2012.07.006 (2012).
78. Parre, E. & Geitmann, A. More than a leak sealant. The mechanical properties of callose in pollen tubes. *Plant Physiol.* **137**, 274–286, doi:10.1104/pp.104.050773 (2005).
79. Hirota, K. *et al.* Nucleoredoxin, glutaredoxin, and thioredoxin differentially regulate NF- κ B, AP-1, and CREB activation in HEK293 cells. *Biochem. Biophys. Res. Commun.* **274**, 177–182, doi:10.1006/bbrc.2000.3106 (2000).
80. Lechward, K. *et al.* Interaction of nucleoredoxin with protein phosphatase 2A. *FEBS Lett.* **580**, 3631–3637, doi:10.1016/j.febslet.2006.04.101 (2006).
81. Muller, L., Funato, Y., Miki, H. & Zimmermann, R. An interaction between human Sec63 and nucleoredoxin may provide the missing link between the SEC63 gene and polycystic liver disease. *FEBS Lett.* **585**, 596–600, doi:10.1016/j.febslet.2011.01.024 (2011).
82. Qin, Y. *et al.* Penetration of the stigma and style elicits a novel transcriptome in pollen tubes, pointing to genes critical for growth in a pistil. *PLoS Genet.* **5**, e1000621, doi:10.1371/journal.pgen.1000621 (2009).
83. Arif, S. A. *et al.* Isolation and characterization of the early nodule-specific protein homologue (Hev b 13), an allergenic lipolytic esterase from *Hevea brasiliensis* latex. *J. Biol. Chem.* **279**, 23933–23941, doi:10.1074/jbc.M309800200 (2004).
84. Roshal, S., Schmidt, R., Schell, J. & Wilmitzer, L. Isolation and characterization of a gene from *Solanum tuberosum* encoding patatin, the major storage protein of potato tubers. *Mol. Gen. Genet.* **203**, 2144–2220 (1986).
85. Racusen, D. Lipid acyl hydrolase activity of patatin. *Can. J. Bot.* **62**, 154–164, doi:10.1139/b84-220 (1984).
86. Jekel, P. A., Hofsteenge, J. & Beintema, J. J. The patatin-like protein from the latex of *Hevea brasiliensis* (Hev b 7) is not a vacuolar protein. *Phytochemistry* **63**, 517–522, doi:10.1016/S0031-9422(03)00224-3 (2003).
87. Kostyal, D. A., Hickey, V. L., Noti, J. D., Sussman, G. L. & Beezhold, D. H. Cloning and characterization of a latex allergen (Hev b 7): homology to patatin, a plant PLA2. *Clin. Exp. Immunol.* **112**, 355–362, doi:10.1046/j.1365-2249.1998.00596.x (1998).
88. Wang, Y., Wu, H. & Yang, M. Microscopy and bioinformatic analyses of lipid metabolism implicate a sporophytic signaling network supporting pollen development in Arabidopsis. *Mol. Plant* **1**, 667–674, doi:10.1093/mp/ssn027 (2008).
89. Paparella, C., Savatin, D. V., Marti, L., De Lorenzo, G. & Ferrari, S. The Arabidopsis LYSIN MOTIF-CONTAINING RECEPTOR-LIKE KINASE3 regulates the cross talk between immunity and abscisic acid responses. *Plant Physiol.* **165**, 262–276, doi:10.1104/pp.113.233759 (2014).

90. Smit, P. *et al.* Medicago LYK3, an entry receptor in rhizobial nodulation factor signaling. *Plant Physiol.* **145**, 183–191, doi:10.1104/pp.107.100495 (2007).
91. Haney, C. H. *et al.* Symbiotic rhizobia bacteria trigger a change in localization and dynamics of the Medicago truncatula receptor kinase LYK3. *The Plant Cell* **23**, 2774–2787, doi:10.1105/tpc.111.086389 (2011).
92. Verica, J. A., Chae, L., Tong, H., Ingmire, P. & He, Z. H. Tissue-specific and developmentally regulated expression of a cluster of tandemly arrayed cell wall-associated kinase-like genes in Arabidopsis. *Plant Physiol.* **133**, 1732–1746, doi:10.1104/pp.103.028530 (2003).
93. Diener, A. C. & Ausubel, F. M. Resistance to Fusarium Oxysporum 1, a dominant Arabidopsis disease-resistance gene, is not race specific. *Genetics* **171**, 305–321, doi:10.1534/genetics.105.042218 (2005).
94. Meier, S. *et al.* The Arabidopsis wall associated kinase-like 10 gene encodes a functional guanylyl cyclase and is co-expressed with pathogen defense related genes. *PLoS One* **5**, e8904, doi:10.1371/journal.pone.0008904 (2010).
95. Hasslacher, M. *et al.* High-level intracellular expression of hydroxynitrile lyase from the tropical rubber tree Hevea brasiliensis in microbial hosts. *Protein Express. Purif* **11**, 61–71, doi:10.1006/prep.1997.0765 (1997).
96. Schluter, U. *et al.* Recombinant protease inhibitors for herbivore pest control: a multitrophic perspective. *J. Exp. Bot.* **61**, 4169–4183, doi:10.1093/jxb/erq166 (2010).
97. Glazer, A. N., Barel, A. O., Howard, J. B. & Brown, D. M. Isolation and characterization of fig lysozyme. *J. Biol. Chem.* **244**, 3583–3589 (1969).
98. Howard, J. B. & Glazer, A. N. Studies of the physicochemical and enzymatic properties of papaya lysozyme. *J. Biol. Chem.* **242**, 5715–5723 (1967).
99. Lynn, K. R. Four lysozymes from the latex of *Asclepias syriaca*. *Phytochemistry* **28**, 1345–1348, doi:10.1016/S0031-9422(00)97743-4 (1989).
100. Agrawal, A. A. & Konno, K. Latex: a model for understanding mechanisms, ecology, and evolution of plant defense against herbivory. *Annu. Rev. Ecol. Evol. Syst.* **40**, 311–331, doi:10.1146/annurev.ecolsys.110308.120307 (2009).
101. Martin, M. N. The latex of *Hevea brasiliensis* contains high levels of both chitinases and chitinases/lysozymes. *Plant Physiol.* **95**, 469–476, doi:10.1104/pp.95.2.469 (1991).
102. Tan, D. *et al.* Identification of an endophytic antifungal bacterial strain isolated from the rubber tree and its application in the biological control of banana fusarium wilt. *PLoS One* **10**, e0131974 (2015).
103. Kalbe, C., Marten, P. & Berg, G. Strains of the genus *Serratia* as beneficial rhizobacteria of oilseed rape with antifungal properties. *Microbiol. Res.* **151**, 433–439, doi:10.1016/S0944-5013(96)80014-0 (1996).
104. Wang, K. *et al.* Potential of chitinolytic *Serratia marcescens* strain JPP1 for biological control of *Aspergillus parasiticus* and Aflatoxin. *Biomed Res. Int* **2013**, 397142, doi:10.1155/2013/397142 (2013).
105. Someya, N. *et al.* Co-inoculation of an antibiotic-producing bacterium and a lytic enzyme-producing bacterium for the biocontrol of tomato wilt caused by *Fusarium oxysporum* f. sp. *lycopersici*. *Biocontrol Sci.* **12**, 1–6, doi:10.4265/bio.12.1 (2007).
106. Kramer, K. J. & Muthukrishnan, S. Insect chitinases: molecular biology and potential use as biopesticides. *Insect Biochem. Mol. Biol.* **27**, 887–900, doi:10.1016/S0965-1748(97)00078-7 (1997).
107. Kabir, K. E. *et al.* Effect of *Bombyx mori* chitinase against Japanese pine sawyer (*Monochamus alternatus*) adults as a biopesticide. *Biosci. Biotechnol. Biochem.* **7**, 219–229, doi:10.1271/bbb.70.219 (2006).
108. Kim, J. S. *et al.* Isolation of stress-related genes of rubber particles and latex in fig tree (*Ficus carica*) and their expressions by abiotic stress or plant hormone treatments. *Plant Cell Physiol* **44**, 412–414, doi:10.1093/pcp/pcg058 (2003).
109. Azarkan, M., Wintjens, R., Looze, Y. & Baeyens-Volant, D. Detection of three wound-induced proteins in papaya latex. *Phytochemistry* **65**, 525–534, doi:10.1016/j.phytochem.2003.12.006 (2004).
110. Lawrence, S. D. & Novak, N. G. Expression of poplar chitinase in tomato leads to inhibition of development in Colorado potato beetle. *Biotechnol. Lett.* **28**, 593–599, doi:10.1007/s10529-006-0022-7 (2006).
111. Kush, A., Goyvaerts, E., Chye, M. L. & Chua, N. H. Laticifer-specific gene expression in *Hevea brasiliensis* (rubber tree). *Proc. Natl. Acad. Sci. USA* **87**, 1787–1790, doi:10.1073/pnas.87.5.1787 (1990).
112. Jacob, J. L. *et al.* The biological mechanism controlling *Hevea brasiliensis* rubber yield. *Plantation Recherche De'veloppement* **5**, 14–16 (1998).
113. Tan, D., Sun, X. & Zhang, J. Histochemical and immunohistochemical identification of laticifer cells in callus cultures derived from anthers of *Hevea brasiliensis*. *Plant Cell Rep* **30**, 1117–1124, doi:10.1007/s00299-011-1019-9 (2011).
114. Tan, D., Sun, X. & Zhang, J. Age-dependent and jasmonic acid-induced laticifer-cell differentiation in anther callus cultures of rubber tree. *Planta* **240**, 337–344, doi:10.1007/s00425-014-2086-2 (2014).
115. Tang, C., Qi, J., Li, H., Zhang, C. & Wang, Y. A convenient and efficient protocol for isolating high-quality RNA from latex of *Hevea brasiliensis* (para rubber tree). *J. Biochem. Biophys. Methods* **70**, 749–754, doi:10.1016/j.jbbm.2007.04.002 (2007).
116. Altschul, S. F. *et al.* Gapped BLAST and PSI-BLAST: a new generation of protein database search programs. *Nucleic Acids Res* **25**, 3389–3402, doi:10.1093/nar/25.17.3389 (1997).
117. Roberts, A. *Ambiguous fragment assignment for high-throughput sequencing experiments* Ph. D thesis, University of California, Berkeley (2013).
118. Robinson, M. D. & Oshlack, A. A scaling normalization method for differential expression analysis of RNA-seq data. *Genome Biol.* **11**, R25, doi:10.1186/gb-2010-11-3-r25 (2010).
119. Dillies, M. A. *et al.* A comprehensive evaluation of normalization methods for Illumina high-throughput RNA sequencing data analysis. *Brief Bioinform.* **14**, 671–683, doi:10.1093/bib/bbs046 (2013).
120. Young, M. D., Wakefield, M. J., Smyth, G. K. & Oshlack, A. Gene ontology analysis for RNA-seq: accounting for selection bias. *Genome Biol.* **11**, R14, doi:10.1186/gb-2010-11-2-r14 (2010).
121. Usadel, B., Porée, F., Nagel, A. & Stitt, M. A guide to using MapMan to visualize and compare Omics data in plants: a case study in the crop species, Maize. *Plant Cell Environ* **32**, 1211–1229, doi:10.1111/pce.2009.32.issue-9 (2009).
122. Bustin, S. A. *et al.* The MIQE guidelines: minimum information for publication of quantitative real-time PCR experiments. *Clin. Chem.* **55**, 611–622, doi:10.1373/clinchem.2008.112797 (2009).
123. Li, H., Qin, Y., Xiao, X. & Tang, C. Screening of valid reference genes for real-time RT-PCR data normalization in *Hevea brasiliensis* and expression validation of a sucrose transporter gene HbSUT3. *Plant Sci.* **181**, 132–139, doi:10.1016/j.plantsci.2011.04.014 (2011).
124. Deng, W., Wang, Y., Liu, Z., Cheng, H. & Xue, Y. HemI: a toolkit for illustrating heatmaps. *PLoS One* **9**, e111988, doi:10.1371/journal.pone.0111988 (2014).
125. Livak, K. J. & Schmittgen, T. D. Analysis of relative gene expression data using real-time quantitative PCR and the $2^{-\Delta\Delta Ct}$ Method. *Methods* **25**, 402–408, doi:10.1006/meth.2001.1262 (2001).

Acknowledgements

This project was funded by the Natural Science Foundation of China under grant number 31471561.

Author Contributions

J.Z. and D.T. conceived the study; D.T., A.K., L.F. and X.S. performed morphological studies and isolated RNA; X.H. and Z.D. performed bioinformatic analysis. L.F. performed qRT-PCR analysis. J.Z. wrote the main manuscript text and prepared Figs S1–2 and 4–8. X.H. prepared Fig. 3. Z.D. prepared Supplementary Figs S1, S2, and S3. All authors reviewed the manuscript.

Additional Information

Supplementary information accompanies this paper at doi:[10.1038/s41598-017-03083-3](https://doi.org/10.1038/s41598-017-03083-3)

Competing Interests: The authors declare that they have no competing interests.

Accession codes: The transcriptome data has been submitted to NCBI database under accession number SRP095295.

Publisher's note: Springer Nature remains neutral with regard to jurisdictional claims in published maps and institutional affiliations.



Open Access This article is licensed under a Creative Commons Attribution 4.0 International License, which permits use, sharing, adaptation, distribution and reproduction in any medium or format, as long as you give appropriate credit to the original author(s) and the source, provide a link to the Creative Commons license, and indicate if changes were made. The images or other third party material in this article are included in the article's Creative Commons license, unless indicated otherwise in a credit line to the material. If material is not included in the article's Creative Commons license and your intended use is not permitted by statutory regulation or exceeds the permitted use, you will need to obtain permission directly from the copyright holder. To view a copy of this license, visit <http://creativecommons.org/licenses/by/4.0/>.

© The Author(s) 2017